Proceedings of the IASS 2024 Symposium
Redefining the Art of Structural Design
August 26-30, 2024, Zurich, Switzerland
Philippe Block, Giulia Boller, Catherine DeWolf,
Jacqueline Pauli, Walter Kaufmann (eds.)

Integrating Shape and Topology Optimization:A Multi-Stage Design Approach for Shell Structures

Saaranya Kumar DASARI*, Patrizia TROVALUSCI[a], Nicholas FANTUZZI[b], Marco PINGARO[a]

* [a] Sapienza University of Rome
DISG Department, Via Antonio Gramsci 53, Rome, Italy
saaranyakumar.dasari@uniroma1.it

[b] University of Bologna, DICAM Department, Bologna, Italy

Abstract

This paper introduces an innovative methodology for optimizing the shape and topology of shell structures, adopting Dynamic Relaxation along with the Solid Isotropic Material with Penalization (SIMP) method. Dynamic Relaxation is harnessed as a powerful tool for versatile shape refinement, enabling a thorough exploration of diverse design possibilities [1]. Following this, the SIMP method is applied to identify optimal material layouts within the structure [2], emphasizing the most effective arrangement that reinforces the shell structure while minimizing overall material usage [3]. The Method of Moving Asymptotes (MMA) is utilized to facilitate a series approximation to the constraint function, resolving sub-problems and enhancing the optimization process. In addition to these methodologies, the paper incorporates considerations of Global Warming Potential (GWP) and buildability, addressing the practical feasibility and ease of construction. This approach offers a clear pathway toward the creation of sustainable spatial structures, aligning with environmental responsibility in the face of climate change challenges. By providing a concise yet comprehensive exploration of shape and material optimization, our approach establishes a framework for the development of spatial structures that not only exhibit structural efficiency but also contribute to environmental sustainability.

Keywords: Sustainable Design, Dynamic Relaxation, Topology Optimization, Global Warming Potential, Buildability

1. Introduction

The built environment is responsible for approximately 40% of global greenhouse gas emissions, highlighting the crucial role of the construction sector in mitigating climate change [4]. Traditional methods often lead to excessive material usage and high environmental footprints.The construction industry's significant contribution to global carbon emissions and resource depletion emphasizes the critical necessity for a shift towards sustainable practices.

In the realm of spatial structures, the intricate relationship between form and structure is particularly pronounced in thin shell structures, where the shape intricately influences force distribution and vice versa. Consequently, designing such structures often involves a two-step process: form-finding followed by structural analysis incorporating material properties and distribution [5]. The complex geometry and curved shapes of these structures require careful and precise formwork, leading to higher construction costs and increased complexity. Specifically for shell structures, the shell must be built twice: first in timber, as custom-built formwork, and then in concrete [6]. When considering the environmental impact of shell structures, it comprises two components: the embodied impact of the structural material and the

impact associated with the actuation control process. In response to these challenges, integrated design approaches incorporating shape and topology optimization have emerged as crucial strategies. With the growing demand for sustainable construction, these integrated approaches not only improve material efficiency but also address the need for environmentally conscious design.

Shape optimization and topology optimization represent critical areas of research in the design of shell structures, encompassing various methodologies such as homogenization [2, 7], SIMP [8]to efficiently perform across a wide range of problems. Significant advancements have been achieved in structural topology optimization over recent decades, leading to increased adoption of this adaptable technique across various research and industrial domains. Previous studies have explored both in-plane and out-of-plane optimization strategies, with a crucial consideration being whether changes in shell surface curvatures are permitted during optimization. For instance, Ansola et al. [3] proposed a method that alternated between shape and topology optimization steps until convergence was achieved. Hassani et al. [9] simultaneously optimized shape and topology parameters in each iteration. Jiang et al. [10] developed an explicit optimization approach based on the moving morphable component method, enabling simultaneous optimization. However, many of these methods were not initially tailored for architectural design, where predefined shapes are common. So, we propose an integrated framework that combines shape and topology optimization algorithms to optimize the shape and material layout of shell structures while considering GWP and buildability Fig1.

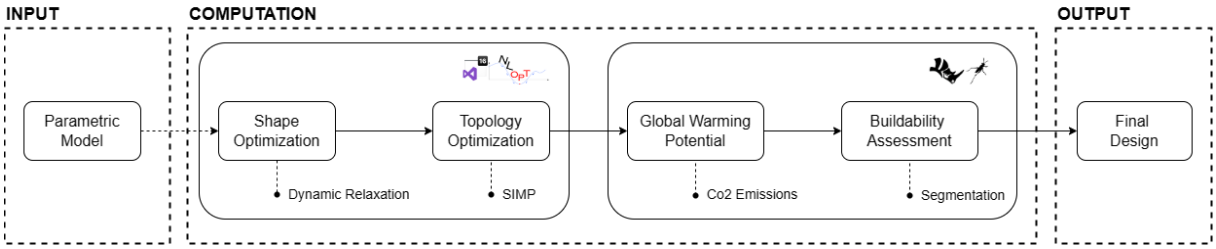

Figure 1: The frame work of the study

In shell topology optimization, we can improve structural performance by incorporating stiffening elements such as ribbed structures [11] or utilizing multi-material shells, this involves strategically placing high-strength materials in regions where additional material strength is needed. Our investigation builds upon this understanding by proposing an integrated approach where shape and topology optimization steps are sequentially conducted using DR and SIMP methods. To enhance our methodology, we incorporate the MMA algorithm [12], leveraging design sensitivity analysis to distinguish our work from previous methods. Following the optimization process, we evaluate the designed structures against GWP and buildability criteria, ensuring their prioritization alongside structural performance metrics. GWP serves as a vital metric for assessing the environmental impact of optimized shell structures, involving quantification of greenhouse gas emissions associated with the production, transportation, and assembly of construction materials [4]. Rationalization, on the other hand, involves breaking down continuous surfaces into discrete panels or elements[13]. This process streamlines design and construction processes by facilitating rationalization, simplification, and standardization. By integrating optimization and segmentation techniques, designers can optimize not only the overall form and material distribution but also the layout and arrangement of individual components. This holistic approach enables consideration of both macroscopic and microscopic design factors, ultimately leading to more comprehensive and efficient solutions.

2. Dynamic relaxation

Dynamic Relaxation, invented by Alistair Day in 1965, initially developed for frame analysis and later extended to address nonlinear equilibrium. DR tracks the structural motion over time under applied loads, incrementally reaching static equilibrium by tracing node motion through explicit time increments, ultimately converging to a steady-state solution equivalent to the static equilibrium solution [1]. We adopted DR formulation from [1, 14] and implemented a python code in visual studio. The code begins by reading an OBJ file representing a 10×10 initial state of system exported from CAD (Rhino) Fig2. It then initializes lists to store various data types and sets up parameters required for DR simulation, including XYZ coordinates, vertex indices, and fixed vertices.

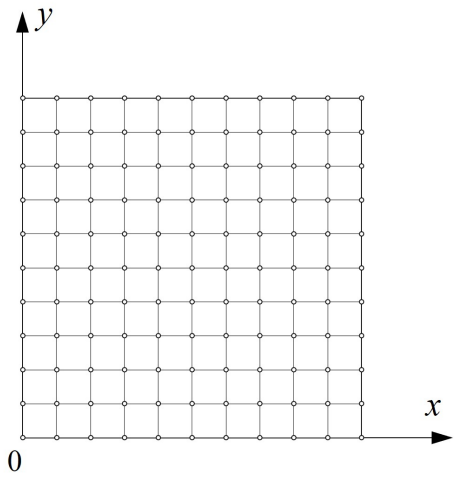

Figure 2: The initial state of the system.

The DR formulation relies on Newton's second law, governing the motion of any node i in the x-direction at time t.

$$M\ddot{u} + C\dot{u} + Ku = F \tag{1}$$

Where, M represent the mass matrix, C the damping matrix and K the stiffness matrix. The variables u and its derivatives represent displacement, velocity, and acceleration.

For each coordinate x,y, or z we do the followings:

$$P_{ix} - K_{ix}\delta_{ix}^{t} - C_i v_{ix}^{t} = M_i \dot{v}_{ix}^{t} \tag{2}$$

$$R_{ix}^{t} = P_{ix} - K_{ix}\delta_{ix}^{t} = M_i \dot{v}_{ix}^{t} + C_i v_{ix}^{t} \tag{3}$$

At node i in direction x at time t, P_{ix} represents the applied force, R_{ix}^{t} the residual of the applied forces, δ_{ix}^{t} the total displacement, C_i the viscous damping constant, v_{ix}^{t} the velocity, M_i indicates the lumped fictitious mass to optimize convergence, and $\dot{v}_{ix}^{t}$ denotes the acceleration.

Acceleration as an approximate derivative of velocity, it signifies the velocity of a specific moment in time by averaging two half-instances just before and after.

$$\dot{v}_{ix}^{t} = \frac{v_{ix}^{t+\Delta t/2} - v_{ix}^{t-\Delta t/2}}{\Delta t} \tag{4}$$

$$v_{ix}^{t} = \frac{v_{ix}^{t+\Delta t/2} + v_{ix}^{t-\Delta t/2}}{\Delta t} \tag{5}$$

By substituting eq(4) & eq(5) in eq(3) and considering that the damping is proportionate to masses $C_i = M_i C$, we have:

$$v_{ix}^{t+\Delta t/2} = A\frac{\Delta t}{M_i} R_{ix}{}_{i}^{t} + B v_{ix}^{t-\Delta t/2} \tag{6}$$

Where, $A = (1/1 + C\Delta t)$ and $B = (1 - C\Delta t/1 + C\Delta t)$ and C is constant. Now, we can use the velocities of the nodes to predict the next position in the system.

$$v_{ix}^{t+\Delta t/2} = \frac{x_i^{t+\Delta t} - x_i^{t}}{\Delta t} \tag{7}$$

$$x_i^{t+\Delta t} = x_i^{t} + v_{ix}^{t+\Delta t/2}\Delta t \tag{8}$$

After obtaining the updated geometry, the new forces can be calculated and integrated with the applied gravity load components P_{ix} to yield the updated residuals.

$$R_{ix}^{t} = P_{ix} + \sum_{i\ j} \left(\frac{f_{i,j}}{l_{i,j}}\right)^{t} x_i - x_j{}^{t} \tag{9}$$

Where, t denotes a time step indicator, f_{ij} represents the elasticity force along the edge (i, j), and l_{ij} is the length of that edge. The division by this length in every direction provides the corresponding shadow. The forces along the edges of the mesh are computed with respect to their rest lengths, given by $f_{ij} = K\Delta l$. After computing residual force, velocities and updating the coordinates using eq(8), we get the final system Fig3.

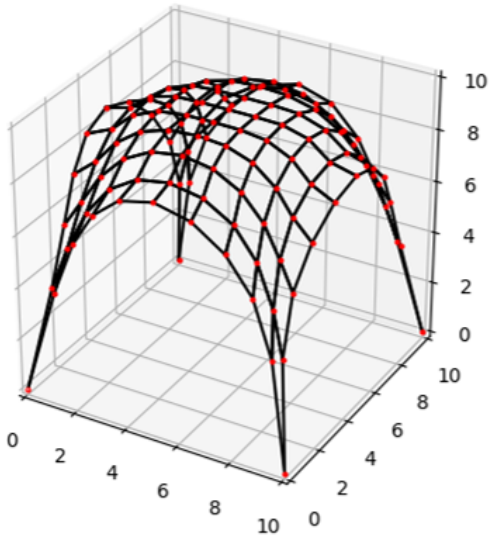

Figure 3: The final state of the system

3. Topology optimization

We use topology optimization to determine the material layout that enhances the stiffness of a structure, this process involves minimizing compliance within a specified design domain. We adopt a straightforward formulation outlined in [2], which involves minimizing output displacement while adhering to a single linear constraint on material usage. We consider linear isotropic materials, and the Young's modulus of an element is determined by the modified SIMP interpolation scheme:

$$E_e = E(\rho_e) = E_{min} + \rho_e^p(E_0 - E_{min}), \quad \rho_e \in [0, 1] \tag{10}$$

Here, p is the penalization power, E_{min} is the stiffness of soft (void) material (kept non-zero to avoid singularity of the stiffness matrix), and E_0 is the Young's modulus of solid material.

The use of the modified SIMP scheme offers several advantages over the standard SIMP scheme, including independence of the minimum stiffness value from the penalization factor, coverage of two-phase design problems, and easier generalization for use in various filtering schemes. Test structures are discretized using 4-node bi-linear finite elements. The implementation is carried out in python, following the methodology described in [8, 15]. For optimization, we utilize the MMA [12], by incorporating the NLopt [16] and autograd [17] python libraries. We examine a test case from [18], this example involves a multiple load points within a design domain Fig 4.

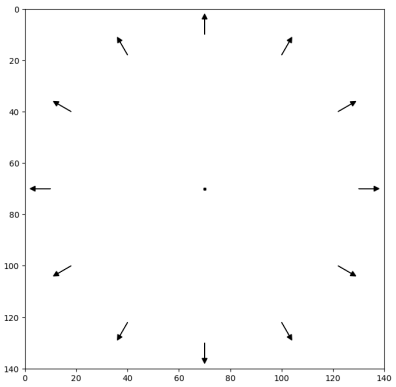

Figure 4: Directions of the applied external forces at multiple points

3.1. Density filters

Density filters operate by adjusting the element density, thereby altering the stiffness based on the densities within a specified neighborhood of an element. The adjusted element density can be expressed as $\tilde{\rho}_e = \tilde{\rho}_e(\rho_i \in N_e)$, meaning that the modified element density $\tilde{\rho}_e$ is determined by the neighboring design variables $\rho_i \in N_e$. Consequently, the modified stiffness in element e can be represented as

$$E_e = E_e(\rho) = E_e(\tilde{\rho}_e) = E_{min} + \tilde{\rho}_e^p(E_0 - E_{min}) \tag{11}$$

where $\tilde{\rho}_e$ denotes the filtered density. An essential feature of filter operators is volume preservation, ensuring that the volume of material remains consistent before and after the filtering process. However, achieving exact volume preservation is rarely feasible in practice due to boundary influences.

3.2. Objective function

At a fundamental level, the optimal structure is one that minimizes the elastic potential energy or compliance of the 2D grid composed of springs. This concept can be expressed mathematically as:

$$\begin{aligned} \text{minimize } \boldsymbol{\rho} : c(\boldsymbol{\rho}) &= \mathbf{U}^T\mathbf{K}\mathbf{u} = \sum_{e=1}^{N_e} E_e(\rho_e)\mathbf{u}_e^T\mathbf{K}_0\mathbf{u}_e \\ \text{Subjected to: } V(\rho)/V_0 &= f \quad \text{A fixed quantity of material} \\ \mathbf{KU} &= \mathbf{F} \quad \text{Hooke's Law} \\ 0 \leq \rho &\leq 1 \quad \text{Densities} \end{aligned} \tag{12}$$

The compliance denoted by c encompasses the material densities represented by the vector $\boldsymbol{\rho}$, the global stiffness matrix $\mathbf{K}$, displacements of the nodes contained in the vector $\mathbf{U}$, and Young's modulus E_e. External forces, or loads, are described by the vector $\mathbf{F}$. The central aspect of this objective, expressed as $c(\boldsymbol{\rho}) = \mathbf{U}^T\mathbf{K}\mathbf{U}$, can be formulated as a high-level objective function that invokes a series of subroutines.

3.2.1. Computing sensitivities

The objective function gives a single value, $c(\boldsymbol{\rho})$, which serves as a metric for assessing the quality of our structure but how do we adjust $\boldsymbol{\rho}$ to minimize this metric. To address this, we must compute the gradients or sensitivities of c concerning $\boldsymbol{\rho}$ based on filtered densities. These sensitivities indicate the direction in which $\boldsymbol{\rho}$ should be adjusted to reduce c as much as possible. If we keep filtering aside and apply the chain rule to the first line of the objective function, we derive:

$$\frac{\partial c}{\partial \rho_e} = -p\rho_e^{p-1}(E_0 - E_{\text{min}})u_e^T K_0 u_e \tag{13}$$

3.3. Optimization

Compliance: At a high level, compliance is represented by $U^T K U$. However, since U and K are very sparse, it's more efficient to compute $\sum_{e=1}^{N_e} E_e(\rho_e)u_e^T K_0 u_e$. This vectorized computation significantly speeds up the process compared to using a for loop. The compliance, being the sum of potential energies of all finite elements, scales each term by $E_e(\rho_e)$ because the stiffness matrix varies with Young's modulus, which depends on the local material density.

Element stiffness matrix: The variable K_0 in the compliance calculation is known as the element stiffness matrix. Conceptually, it's analogous to the spring constant k in a simple harmonic oscillator but extended to 2D. It accounts for all interaction terms between the corner nodes in a square finite element. When we represent the displacements of these nodes with a vector $u = [u_1^a, u_2^a, u_1^b, u_2^b, u_1^c, u_2^c, u_1^d, u_2^d]$, the potential energy of the system can be calculated as $PE = \frac{1}{2}u^T K_0 u$, analogous to the 1D harmonic oscillator potential energy $PE = \frac{1}{2}kx^2$.

Material constants: Two material constants affect the element stiffness matrix. Firstly, Young's modulus measures material stiffness, representing the distortion per unit of force. Mathematically, it's the ratio of tensile stress to tensile strain. Secondly, the Poisson coefficient quantifies perpendicular contraction due to stretching. It's the ratio between lateral contraction per unit length and longitudinal extension. Both coefficients influence the element stiffness matrix construction.

Calculating displacements: Calculating node displacements involves solving the matrix equation $F = KU$, where F is the force vector and U is the displacement vector. With N nodes, each with 2 degrees of freedom, K is a $2N \times 2N$ matrix, resulting in a system of simultaneous linear equations.

Finally,the MMA method handles nonlinear inequality constraints and scales well to large parameter spaces. In the implementation, we rewrite the mass conservation constraint as a mass threshold inequality and set density constraints using upper and lower bounds. Gradients with respect to the objective are computed using Autograd and passed to the NLopt solver, simplifying the optimization process. Ultimately, this process gives the optimal material layout for the specified design domain Fig5.

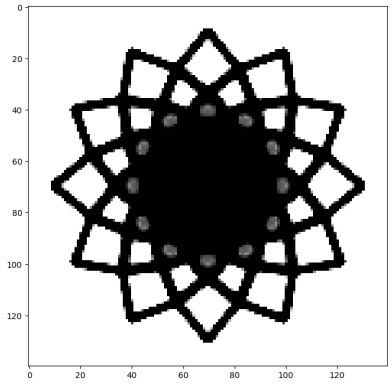

Figure 5: Optimal layout

4. Global warming potential

Greenhouse Gas (GHG) refers to the gases that contribute to global warming, and GHG emissions are often measured in carbon dioxide equivalent (kgCO_2e). GWP[CO_2e] quantifies the contribution of construction activities to climate change by comparing their greenhouse effect over 100 years to that of equivalent CO_2. The overall carbon footprint is the sum of emissions over the entire building life [4].

$$\begin{aligned} &\sum \text{structural elements} \left[\text{Quantity (kg)} \times \text{CO}_2\text{e Material Factor (kg CO}_2\text{e/kg)}\right] \\ &= \text{GWP building (kg CO}_2\text{e)} \end{aligned} \tag{14}$$

When dealing with single-material structures, reducing the volume or weight of the structure can be seen as a means to lessen its environmental footprint. This is because a lighter structure typically entails lower energy consumption and fewer GHG emissions during the material production phase [19].In the context of multi-material structures, simply minimizing structural volume or weight doesn't necessarily correspond to reducing environmental impact. This is because various materials used in such structures may have different densities, energy intensities, and GHG emission coefficients. Here, the environmental impact of a structure refers to the energy consumption or GHG emissions incurred by the structure over its operational lifespan.

For example, if we consider a concrete shell with a thickness of 60 mm for the shell obtained from DR, the total embodied carbon amounts to 15714.3475 kgCO_2e. This calculation is based on the material Concrete, which has a GWP of 0.8 kgCO_2e/kg [20].We utilized the Cardinal LCA plugin for Grasshopper to represent Fig 6. As outlined earlier, the environmental impact of such a structure comprises two main components: the part related to the structural material and the aspect associated with the actuation mechanism. By integrating GWP assessment into the design process, we empower designers and stakeholders to make environmentally responsible decisions. This proactive consideration of GWP not only

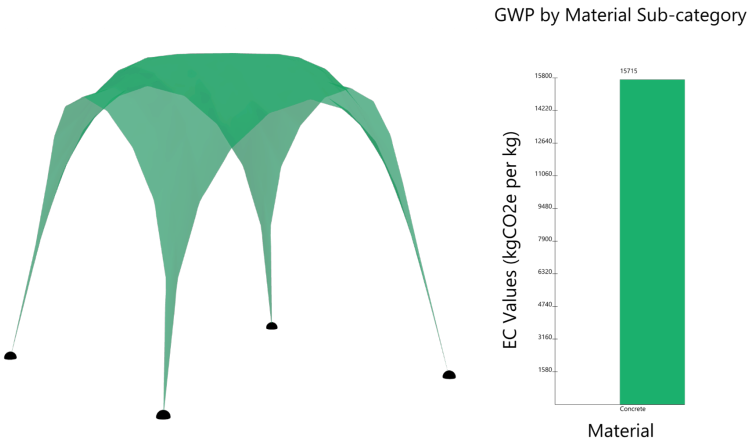

Figure 6: GWP Analysis

allows for the identification of potential environmental impacts but also facilitates the implementation of strategies to mitigate a project's carbon footprint.

5. Buildability

Buildability, defined as the ease of construction and the impact of construction techniques on productivity [21], is a critical aspect of design. It encompasses how construction methods influence efficiency and productivity. Integrating buildability assessments during the design phase can minimize delays, cost overruns, and enhance operational efficiency. Rationalization, essential in construction engineering and product design, is increasingly vital due to complex architectural geometries [22]. Architects often need to adjust designs to fit fabrication constraints, a process known as architectural rationalization [23]. Leveraging machine learning algorithms, like the Gaussian mixture algorithm, can simplify and optimize complex shell geometries for efficient construction. The rationalization of the shell obtained from DR in Fig7 involves clustering based on the area of the panels. This clustering procedure is facilitated using tools such as the Lunch Box ML plugin for Grasshopper.

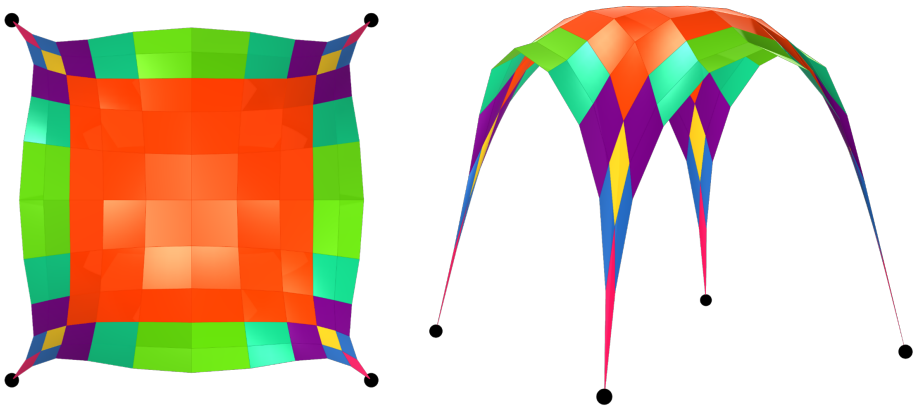

Figure 7: Rationalization

Clustering, a foundational technique in data analysis, organizes unlabelled data points into meaningful clusters based on similarities [24]. In structural architecture, clustering groups structural elements based

on shared attributes, aiding rationalization efforts. The Gaussian Mixture algorithm organizes 3D panel geometries into clusters, supporting design and fabrication activities for complex structures, achieving Gaussian Panel Groupings based on shared dimensional characteristics, which benefit shell structures and rationalization efforts. This unsupervised learning algorithm analyzes geometric attributes to group panels into coherent clusters, aiding subsequent design and fabrication activities.

6. Conclusions and Perspectives

The paper presents an in-depth exploration of the role of integrated design methodologies, including shape and topology optimization, as well as considerations GWP and buildability aspects. The shape obtained from DR enables the construction of a mesh with faces and updates coordinates, seamlessly accommodating the sequence of optimization. It should be noted that while the topology optimization test case addresses only a 2D problem, the introduced formulations are also applicable to 3D scenario. The optimal layout allows us to utilize it either as stiffeners or allocate high strength materials within the shell by leveraging the material efficiency. Although our approach requires further refinement and development, it holds potential for sustainable practices in the construction industry, particularly in spatial structures. This potential lies in the intricate interplay among form, topology, materials associated with GHG emission coefficients ($kgCO_2e/kg$), and rationalization. In conclusion, as the demand for sustainable construction grows, these integrated methodologies unlock new possibilities for structurally efficient and environmentally sustainable spatial structures.

Acknowledgments

The Authors gratefully acknowledge the financial support provided by the PhD Program of Structural and Geotechnical Engineering, Sapienza University of Rome, Italy

References

[1] S. Adriaenssens, P. Block, D. Veenendaal, and C. Williams, *Shell structures for architecture: form finding and optimization*. Routledge, 2014.

[2] M. P. Bendsoe and N. Kikuchi, "Generating optimal topologies in structural design using a homogenization method," *Computer methods in applied mechanics and engineering*, vol. 71, no. 2, pp. 197–224, 1988.

[3] R. Ansola, J. Canales, J. A. Tárrago, and J. Rasmussen, "An integrated approach for shape and topology optimization of shell structures," *Computers Structures*, vol. 80, no. 5, pp. 449–458, 2002, ISSN: 0045-7949.

[4] C. C. E. L. De Wolf, "Low carbon pathways for structural design: Embodied life cycle impacts of building structures," Ph.D. dissertation, Massachusetts Institute of Technology, 2017.

[5] S. K. Dasari, N. Fantuzzi, P. Trovalusci, R. Panei, and M. Pingaro, "Optimal design of a canopy using parametric structural design and a genetic algorithm," *Symmetry*, vol. 15, no. 1, 2023.

[6] S. K. Dasari, P. Trovalusci, N. Fantuzzi, M. Pingaro, and R. Panei, "Sustainable spatial structures: A design approach using shape and topology optimization to minimize environmental impact and improve buildability," in *Shell and Spatial Structures*, S. Gabriele, A. Manuello Bertetto, F. Marmo, and A. Micheletti, Eds., Cham: Springer Nature Switzerland, 2024, pp. 279–288.

[7] G. I. Rozvany, M. Zhou, and T. Birker, "Generalized shape optimization without homogenization," *Structural optimization*, vol. 4, pp. 250–252, 1992.

[8] O. Sigmund, "A 99 line topology optimization code written in matlab," *Structural and multidisciplinary optimization*, vol. 21, pp. 120–127, 2001.

[9] G. H. Hassani Behrooz Tavakkoli Seyed Mehdi, "Simultaneous shape and topology optimization of shell structures," *Structural and Multidisciplinary Optimization*, vol. 48, pp. 221–233, 2013, ISSN: 1615-1488.

[10] X. Jiang, W. Zhang, C. Liu, Z. Du, and X. Guo, "An explicit approach for simultaneous shape and topology optimization of shell structures," *Applied Mathematical Modelling*, vol. 113, pp. 613–639, 2023, ISSN: 0307-904X. DOI: 10.1016/j.apm.2022.09.028.

[11] D. Veenendaal, J. Bakker, and P. Block, "Structural design of the flexibly formed, mesh-reinforced concrete sandwich shell roof of nest hilo," *Journal of the International Association for Shell and Spatial Structures*, vol. 58, no. 1, pp. 23–38, 2017, ISSN: 1028-365X. DOI: 10.20898/j.iass.2017.191.847.

[12] K. Svanberg, "The method of moving asymptotes—a new method for structural optimization," *International Journal for Numerical Methods in Engineering*, vol. 24, no. 2, pp. 359–373, 1987.

[13] R. Oval, "Topology finding of patterns for structural design," Ph.D. dissertation, Université Paris-Est, 2019.

[14] T. V. Mele, *Dynamic relaxation*, https://block.arch.ethz.ch/blog/2014/07/dynamic-relaxation/, Accessed March 2024.

[15] E. Andreassen, A. Clausen, M. Schevenels, B. S. Lazarov, and O. Sigmund, "Efficient topology optimization in matlab using 88 lines of code," *Structural and Multidisciplinary Optimization*, vol. 43, pp. 1–16, 2011.

[16] S. G. Johnson, *The NLopt nonlinear-optimization package*, https://github.com/stevengj/nlopt, 2007.

[17] D. Maclaurin, D. Duvenaud, and R. P. Adams, "Autograd: Effortless gradients in numpy," in *ICML 2015 AutoML Workshop*, vol. 238, 2015, p. 5.

[18] K. Svanberg and H. Svard, "Density filters for topology optimization based on the geometric and harmonic means," in *10th world congress on structural and multidisciplinary optimization. Orlando*, 2013.

[19] X. Xu, J. You, Y. Wang, and Y. Luo, "Analysis and assessment of life-cycle carbon emissions of space frame structures," *Journal of Cleaner Production*, vol. 385, p. 135 521, 2023.

[20] *Embodied carbon footprint database -circular ecology.* https://circularecology.com/embodied-carbon-footprint-database.html, Accessed June 2023.

[21] *Bca,: Code of practice on buildability 2022 edition, 1–105*, https://www1.bca.gov.sg, Accessed May 2023.

[22] Y. Liu, T.-U. Lee, A. R. Javan, N. Pietroni, and Y. M. Xie, "Reducing the number of different faces in free-form surface approximations through clustering and optimization," *Computer-Aided Design*, vol. 166, p. 103 633, 2023.

[23] D. Pellis, M. Kilian, H. Pottmann, and M. Pauly, "Computational design of weingarten surfaces," *ACM Transactions on Graphics (TOG)*, vol. 40, no. 4, pp. 1–11, 2021.

[24] N. Miller and D. Stasiuk, "Negotiating structured building information data," *Design Transactions: Rethinking Information Modelling for a New Material Age*, pp. 68–73, 2020.